Evaluation of the Global Atmospheric Moisture Budget as Seen from Analyses

KEVIN E. TRENBERTH AND CHRISTIAN J. GUILLEMOT

National Center for Atmospheric Research, Boulder, Colorado*

(Manuscript received 18 November 1994, in final form 7 March 1995)

ABSTRACT

For the period 1987 to 1993, quantities central to the global moisture budget from the global analyses of the European Centre for Medium-Range Weather Forecasts (ECMWF), the U.S. National Meteorological Center (NMC), and NASA/Goddard have been computed and compared. The precipitable water is computed and compared with satellite data from the Special Sensor Microwave Imager (SSM/I). Fluxes of moisture and their divergence have been used to estimate the vertically integrated moisture budget and thus evaporation minus precipitation ($E - P$) as residuals. Results of several test computations show that small biases exist in precipitable water as vertical resolution and methods of computing vertical integrals are changed, but the impact is small on the moisture budget. In the Tropics and subtropics the moisture budget is dominated by the divergence field rather than the moisture amounts, and consequently initialization of the analyses has an impact on the perceived moisture budget. The diurnal cycle is shown to be important especially for $E - P$. For the vertically integrated moisture budget, the use of pressure coordinates instead of the model coordinates on which the data are analyzed produces acceptably small differences for the most part, although adequate resolution at low levels and proper treatment of the surface is important. Computations at different horizontal resolutions reveal the importance of adequate resolution in the vicinity of steep orography but also that resolution is not a big factor on large scales even where steep gradients in precipitation exist. The implication is that it is the veracity of the large-scale divergence and moisture fields themselves that contribute to problems, and these arise from the moist physics of the assimilating model used in four-dimensional data assimilation, which dominates the character of the analyses. However, in the subtropics large positive biases are present in precipitable water in the ECMWF and, to a lesser extent, NMC analyses and are partly due to the assimilation of biased TOVS retrievals. The effects of the large and spurious changes in analysis systems at ECMWF and NMC are manifested in the results. Differences between ECMWF and NMC $E - P$ locally are 60%–75% of the values themselves in the Tropics at T31 resolution and about one-half as much at T15 resolution, and they are not diminishing with time. By making use of estimates of E and P from the NASA/Goddard reanalysis, both spatial and temporal variability of $E - P$ are found to be dominated by the P field. Accordingly, for part of 1987 and 1988, estimates of precipitation from the Global Precipitation Climatology Project are used to qualitatively assess the $E - P$ estimates. The ECMWF estimates appear to be best at that time, but since then the NMC values have become less intense while the ECMWF estimates have greatly intensified. The large differences that still exist in such estimates are apt to be carried over to the NMC and ECMWF reanalysis products.

1. Introduction

Moisture is critically important to life on earth, and human welfare and many human activities, especially agriculture, depend upon having just the right amount. Yet it is surprising how poorly the global hydrological cycle is known and how little attention has been given to the causes of major perturbations such as long-term widespread droughts and floods. One source of interannual variability in both is the El Niño–Southern Oscillation (ENSO) phenomenon, which has associated with it extremes of opposite sign in rainfall throughout the Tropics and subtropics (see Glantz et al. 1991 for an overview).

Reasons for the scanty knowledge of both moisture in the atmosphere and precipitation stem from the lack of observations, especially over the oceans, and the nature of the quantities. Rainfall and clouds often occur on quite small time scales and space scales, so that a single moisture or precipitation observation is not representative of a very large area or for more than a small fraction of a day. Moreover, measurements of precipitation occur only where humans live in relatively widely spaced locations, and the buckets used to measure accumulations may not catch it all, especially under snowy and windy conditions. Satellite data on moisture have been made available to the global analyses from TOVS (TIROS Operational Vertical Sounder), although with mixed results (Liu et al. 1992; Wittemeyer and Vonder Haar 1994) as discussed later.

* The National Center for Atmospheric Research is sponsored by the National Science Foundation.

Corresponding author address: Dr. Kevin E. Trenberth, National Center for Atmospheric Research, P.O. Box 3000, Boulder, CO 80307-3000.
E-mail: trenbert@ncar.ucar.edu

After July 1987 fields of precipitable water and other quantities from the Special Sensor Microwave Imager (SSM/I) have become available, but these are not produced in time for operational purposes.

One means of obtaining global fields is from the global analyses resulting from assimilation of observed moisture data into models as part of four-dimensional data assimilation (4DDA)—see section 2. However, this can only occur reliably if the moist physics of the model are realistic; otherwise convective adjustments and cumulus parameterizations are apt to be activated changing the moisture field to one that the model is comfortable with (e.g., see Norquist and Chang 1994). Together with the representiveness issues for observations, these factors have led to little attention being given to moisture fields in the global analyses. The consequence has been that the moisture fields of both relative and specific humidity have changed abruptly every time there is a big change in the 4DDA system, (Trenberth and Olson 1988b; Trenberth 1992). At the European Centre for Medium-Range Weather Forecasts (ECMWF), changes in zonal mean relative humidities of 20% are common, such as when the T106 spectral model was introduced into the 4DDA system on 1 May 1985 (Fig. 1). Major changes also occurred with the introduction of changes in the model physics on 2 May 1989 and 4 August 1993. Most of the main features in Fig. 1 are also spurious and can be identified with system changes, although at times the effects are seen more at other levels (see Trenberth 1992). Because moisture transport in the Tropics is so dependent on the divergent part of the wind field, which has also undergone major changes with time, Fig. 1 also presents the changes in the zonal mean Hadley circulation, as given by the meridional wind at 1.4°S. Note the weakness of the Hadley Cell in the early years of operations (1980 to 1982), after which the annual cycle becomes evident, although with the upper branch of the Hadley Cell continuing to strengthen and expand in vertical extent with time with each model change.

An evaluation and comparison of National Meteorological Center (NMC) and ECMWF analyses performed by Trenberth and Olson (1988a,b) dealt with the global analyses through 1986. A purpose of this paper is to carry the comparison through 1993, with a special focus on moisture and the moisture budget, with the latter represented by evaporation E minus precipitation P computed as a residual from the large-scale atmospheric transports. Previously, Rosen and Salstein (1980) revealed serious problems in NMC's operational moisture analyses using NMC's first global 4DDA system, and Rosen and Salstein (1985) found little improvement when they compared NMC and ECMWF moisture fields for 1983. We also include some results from the newly available "reanalysis" by NASA/Goddard (Schubert et al. 1993).

The focus is on an evaluation of the analyses as the "best" depiction of what occurs in the real world. It is

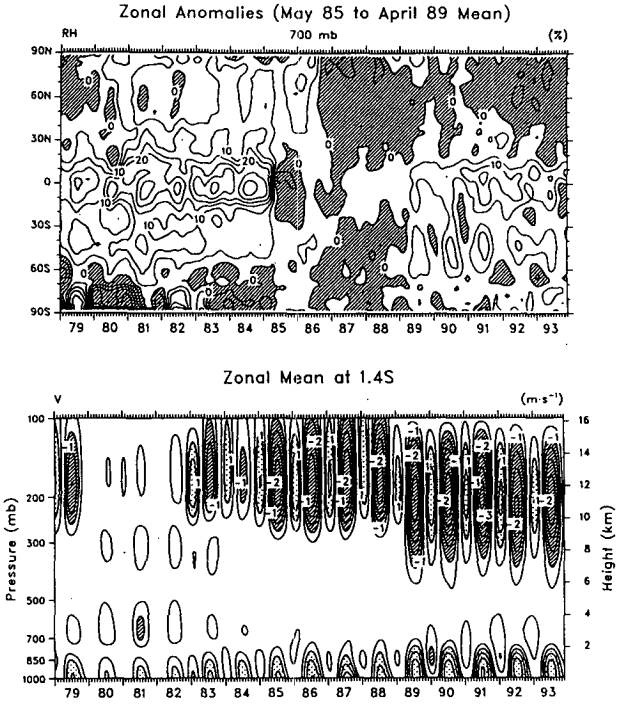

FIG. 1. From ECMWF analyses. (a) Latitude–time section of monthly mean relative humidity zonal mean, departures from the mean annual cycle for May 1985 to April 1989 at 700 mb in percent. The contour interval is 5% and negative departures are shaded. (b) Variations in the upper and lower branches of the Hadley circulation are revealed by the height–time section of monthly mean zonal mean meridional wind at 1.4°S. The contour interval is 0.5 m s^{-1}, the zero contour is omitted, values greater than 1 m s^{-1} are stippled, and values less than -1 m s^{-1} are hatched.

not the main purpose to evaluate the assimilating model and the E and P from these models; however, we make use of some of these fields to clarify the dominant processes, and the results do have implications for the models. The models are imperfect, and the model content of the analyses depends on the data availability. However, the analyses include an analysis increment (or innovation, which is the observation minus background forecast), which should bring the analyses closer to the truth in regions of ample data. Short-term model integrations are often used to provide estimates of E and P, but most models are plagued by a spinup of the hydrological cycle so that the results are not very useful [e.g., Trenberth (1992) presents results for ECMWF and how the spinup has changed with time]. Instead, in these models, values may be taken for intervals as much as 36 h into the forecast to allow transients to die away, but then the model influence is much greater. The incremental analysis update procedure used by NASA/Goddard greatly reduces the initial imbalances and spinup (Schubert et al. 1993), making the E and P estimates from short-term integrations more representative.

The technique for deducing $E - P$ as a residual has a long history, although usually by making use of ra-

winsonde data rather than global analyses. The results of many of these studies are encapsulated by the review of Peixoto and Oort (1983; see also Savijärvi 1988). Most previous studies have not properly accounted for variations in surface pressure p_s, as discussed in Trenberth (1991). Recent examples using global analyses are by Roads et al. (1992, 1994) for NMC data and Oki et al. (1993) for ECMWF data.

It has been suggested that the global atmospheric analyses may have too low horizontal and vertical resolution to properly represent small-scale hydrological processes (Mo and Rasmusson 1990). For example, a nocturnal low-level jet confined to the lowest kilometer of the atmosphere as part of a strong diurnal variation has been shown to play a leading role in the moisture budget of the United States through the strong moisture transport into the Great Plains across the Gulf Coast (Helfand and Schubert 1995). A key question to be addressed is the extent to which horizontal and vertical resolutions in the analyses are an issue versus the ability of the model used in 4DDA to adequately depict the moist processes.

The large number of datasets used in this study are introduced in section 2. Section 3 describes the methodology, and a number of test computations for one month of precipitable water and $E - P$ are described in section 4. These include tests for vertical and horizontal resolution, initialization, twice versus four-times daily data, model versus pressure-level archives, and the source of the data. For 1987 to 1993 the precipitable water comparisons among the ECMWF and NMC analyses and the analyses over the ocean from two different SSM/I algorithms, which are taken to be close to the "truth," are described in section 5. Section 6 describes the comparisons among the $E - P$ estimates and includes a discussion of E and P separately from the NASA/Goddard archive as well, with some measure of "truth" coming from the precipitation fields as provided by the Global Precipitation Climatology Project (GPCP) (Arkin and Xie 1994). The conclusions are given in section 7.

2. Datasets

Global analyses are produced using 4DDA in which multivariate observed data are combined with the "first guess" using a statistically optimum scheme. The first guess is the best estimate of the current state of the atmosphere from previous analyses produced using a numerical weather prediction (NWP) model.

The global atmospheric analyses produced as a result of 4DDA operationally consist of global fields of northward and eastward wind components (u, v), geopotential height (z), temperature (T), and relative humidity (RH), or, equivalently, specific humidity (q) as a function of pressure (p). The ω (= vertical p-velocity) fields are produced diagnostically from the equation of continuity. In recent times, these quantities have been analyzed on the levels of the NWP model used in the 4DDA to provide the first guess for the analyses. Generally, these are σ levels where $\sigma = (p - p_0)/(p_s - p_0)$, where p_s is defined on the model surface topography, and $p_0 = 0$ for most cases but $p_0 = 10$ mb for the NASA/Goddard model. Alternatively, a hybrid between σ and pressure coordinates that typically reverts to constant pressure above about 100 mb is used. Analyzed fields on standard constant pressure levels are produced by interpolation of the changes in the analysis from one synoptic observation time to the next (after November 1984 at ECMWF), though the details as to how this has been done have changed with time. Once the fields have been analyzed, they are typically initialized to bring the mass and temperature fields into a dynamical balance with the velocity fields consistent with the predominant low-frequency motions in the atmosphere.

It must be emphasized that the operational analyses are performed under time constraints for weather forecasting purposes and not for climate purposes. Changes in the NWP model, data-handling techniques, initialization, and so on, which are implemented to improve the weather forecasts, disrupt the continuity of the analyses (Trenberth and Olson 1988b; Trenberth 1992) and impact the moisture fields (Fig. 1).

Several 4DDA datasets have been used, and a summary of their characteristics is given in Table 1. From ECMWF, three datasets are described by Trenberth (1992). The WMO archive from ECMWF consists of seven levels (1000, 850, 700, 500, 300, 200, and 100 mb), is initialized, and covers 1980 to 1989. Two versions of the ECMWF TOGA-WCRP archive exist at NCAR. Both begin in 1985 and are uninitialized; one is from twice-daily data on a 2.5° grid, while the other is four-times daily at T106 resolution. In this notation the "T" refers to triangular truncation at 106 wavenumbers using a spherical harmonic representation. These latter two have analyses at 14 or 15 levels (1000, 925, 850, 700, 500, 400, 300, 250, 200, 150, 100, 70, 50, 30, 10 mb). The 925-mb level became available only from January 1992. All fields are truncated to T42 for processing (Trenberth and Solomon 1993), and a description and evaluation of the ECMWF analyses is given by Trenberth (1992).

An additional dataset from ECMWF is available to us consisting of initialized model level data for one year: July 1990–June 1991. The hybrid-level scheme at ECMWF is described by Simmons and Burridge (1981) and Simmons and Strüfing (1983), and there are 19 model levels available, with five levels below about 850 mb that should help resolve features important for the moisture budget. In addition, as the bottom coordinate corresponds to $p = p_s$, there is no error in computing vertical integrals, although errors are still present from the envelope orography and the discrepancy between the earth's surface and that depicted in the model, as described below. These data

TABLE 1. Summary characteristics of the 4DDA datasets used. Given are the source of the datasets, the horizontal resolution of the archive (latitude–longitude or spectral), the number of vertical layers, whether initialized or not, the number of analyses per day, whether the p_s was recomputed or from the archive, and whether the surface corresponds to a reasonable representation of the real surface or enhanced orography.

Source	Horizontal resolution	Vertical layers	Initialized	Number daily	p_s source	Surface
ECMWF/WMO	2.5 × 2.5	7	Y	2	computed	real
ECMWF/WCRP	2.5 × 2.5	14/15[a]	N	2	computed	real
ECMWF/WCRP	T106	14/15[a]	N	4	computed	real/envelope[b]
ECMWF/hybrid	T106	19	Y	4	archive	envelope
NMC	2.5 × 2.5	12	Y/N[c]	2	computed	real
NASA/Goddard	2.0 × 2.5	20	N	4	archive	real

[a] 15 levels after January 1992.
[b] Real surface for precipitable water but modified envelope for $E - P$.
[c] Not after 25 June 1991.

have been analyzed at full T106 resolution as well as at T42 truncation to determine the effects of the change to lower resolution. This is especially an issue in model coordinates because a change in horizontal resolution is not well defined since the vertical coordinate also changes in the process (Trenberth et al. 1993; Trenberth 1995). In forming time means with these data, variables are weighted with the layer thickness to provide the appropriate mass weighting for vertical integrals to be exact, as described by Trenberth et al. (1993).

For NMC, the analyses are twice daily at 12 levels (1000, 850, 700, 500, 400, 300, 250, 200, 150, 100, 70, 50 mb) on a 2.5° grid. The temperature archived by NMC is virtual temperature, but temperatures at each time have been computed from the available fields. NMC sets RH to zero above 300 mb; therefore the temperature at those levels is unchanged. Missing data have been replaced with ECMWF analyses (in 1987 this was for 35 times, and since then it has averaged nine times per year). All data were interpolated to a T42 grid for processing. An evaluation of earlier NMC data and a comparison with ECMWF data was described by Trenberth and Olson (1988a,b).

Fields of surface pressure p_s were derived for all pressure-level datasets using real mean topography at T42 resolution using methods given in Trenberth (1992). This field is not spectrally truncated. The hydrostatic relation is used if $p_s > 1000$ mb; otherwise interpolation using the geopotential heights is used. The ECMWF analyses include a "surface" pressure field but it does not correspond to the pressure at the real surface of the earth. It is the surface pressure of the model topography, which includes an enhancement as so-called envelope orography. For precipitable water, we used our computed value of p_s as the lower boundary, thereby making use of the extrapolated moisture values below ground. This is done by extrapolating temperatures below ground using an assigned lapse rate and the surface relative humidity to compute a specific humidity (Trenberth et al. 1993). For the ECMWF moisture budget, however, a modified version of the ECMWF-archived p_s was used. A mean difference between ECMWF and real p_s was computed and used to adjust the computed p_s. In this way, spectral Gibbs phenomenon ringing effects from the lower resolution are avoided. For 1985 to 1991 the mean p_s from ECMWF was ~5 mb lower globally (or 17 mb lower over land) than we computed because of envelope orography. Prior to 6 March 1991 NMC also had an enhanced "silhouette" orography, but mean orography has been used since then. However, because there is no archive of the p_s from NMC available, we used our calculated values throughout for both the precipitable water and the moisture budget.

Monthly mean fields of several quantities are also examined from the recent reanalysis by NASA/Goddard (Schubert et al. 1993); see Table 1 for details. Precipitable water is produced from model levels and evaporation and precipitation are accumulated from the NWP model over 3-h increments. The reanalysis covers March 1985 to February 1990, but we have examined data only from 1987 to 1989.

To evaluate the precipitable water over the oceans, we have made use of two sets of monthly mean gridded fields that employ different physically based algorithms applied to SSM/I data from Wentz (see Liu et al. 1992) for July 1987 to June 1991 and from Greenwald and Stephens (hereafter GS; see Greenwald et al. 1993) from July 1987 to December 1991. The former were originally on a 1° grid and the latter on a 2.5° grid. To transform the fields to a T42 grid, an artificial field was first created over land using linear interpolation in the east–west direction, and then values were interpolated to the appropriate Gaussian grid and transformed into spectral space for truncation at T42. Extensive validation of the SSM/I fields by Liu et al. (1992) for the Wentz algorithm prompts us to take these as a measure of the truth. Soden and Bretherton (1994) have compared SSM/I precipitable water for brief periods with ECMWF analyses and other model simulations and cite uncertainties in the satellite product of 2–3 kg m^{-2}.

For precipitation, new global fields becoming available from the GPCP project (Arkin and Xie 1994) consist of a combination of rain gauge data over land and several satellite algorithms over the ocean. It is not the purpose here to explore the accuracy of these fields, but they are regarded as independent measures of P that are useful for evaluating the $E - P$ fields from the other sources because the dominant spatial and temporal variability in $E - P$ originates in P, not E, as will be discussed.

3. Methodology

a. Moisture budget

In the following, use will be made of the equation of state, the hydrostatic equation, and the equation of continuity:

$$\nabla \cdot \mathbf{v} + \frac{\partial \omega}{\partial p} = 0. \tag{1}$$

The vertical mass-weighted integral of the specific humidity, q is the precipitable water w given by

$$w = \int_0^\infty q\rho dz = \frac{1}{g}\int_0^{p_s} q dp. \tag{2}$$

The equation for conservation of water vapor is

$$\frac{\partial q}{\partial t} + \mathbf{v}\cdot\nabla q + \omega\frac{\partial q}{\partial p} = e - c, \tag{3}$$

where e is the rate of reevaporation of cloud and rainwater and c is the rate of condensation per unit mass, which together produce the precipitation rate. The role of liquid water in the atmosphere is ignored. Multiplying (3) by L, the latent heat of vaporization for water gives the latent heat released through evaporation and condensation Q_2 (Yanai et al. 1973). $L(e - c) = -Q_2$ or, using (1), (3) can be expressed in flux form as

$$\frac{\partial q}{\partial t} + \nabla \cdot q\mathbf{v} + \frac{\partial}{\partial p} q\omega = e - c. \tag{4}$$

Using the generic relationships for any A

$$\frac{\partial}{\partial t}\int_0^{p_s} A dp = \int_0^{p_s} \frac{\partial A}{\partial t} dp + A_s \frac{\partial p_s}{\partial t} \tag{5a}$$

$$\nabla \cdot \int_0^{p_s} A\mathbf{v} dp = \int_0^{p_s} \nabla \cdot A\mathbf{v} dp + A_s\mathbf{v}_s \cdot \nabla p_s \tag{5b}$$

$$\int_0^{p_s} \frac{\partial A\omega}{\partial p} dp = A_s\omega_s = A_s\left(\frac{\partial p_s}{\partial t} + \mathbf{v}_s \cdot \nabla p_s\right). \tag{5c}$$

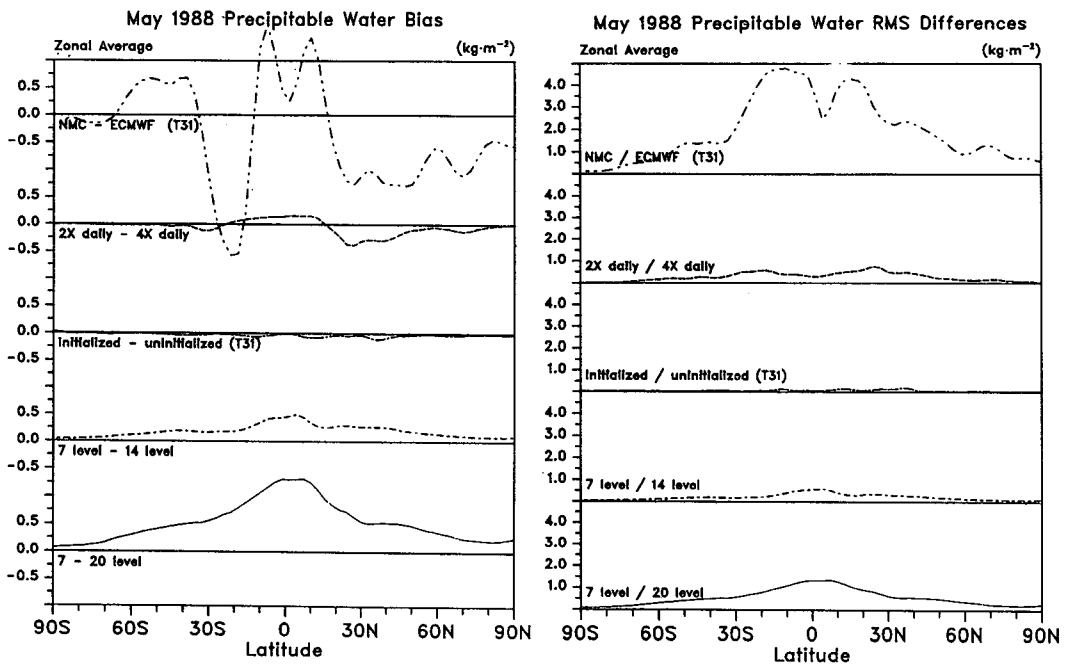

FIG. 2. Results of the tests on precipitable water for May 1988 in kg m^{-2} (= mm). At left are the zonal mean biases and at right the zonal mean rms differences around each latitude circle, where the fields were truncated to T31 before computing the values. In order from top to bottom are NMC–ECMWF, twice versus four times daily, initialized versus uninitialized, 7 versus 14 levels, and 7 versus 20 levels, where the latter uses relative humidity instead of specific humidity for vertical interpolation.

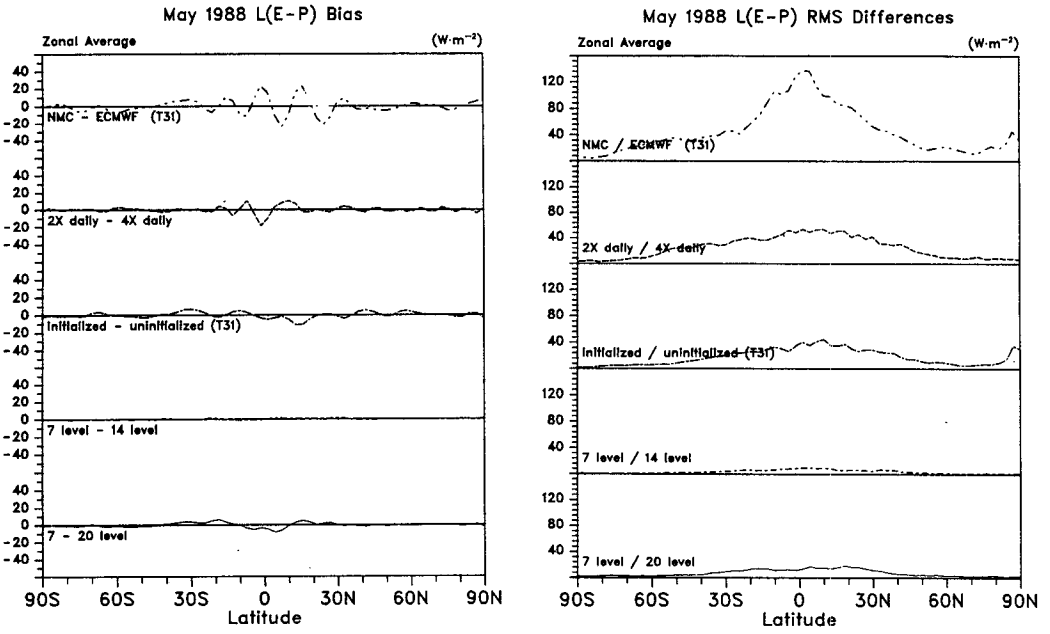

FIG. 3. Results of the tests on $E - P$ for May 1988 multiplied by L so that the units are W m^{-2} (divide by 29 to get mm day^{-1}). At left are the zonal mean biases and at right the zonal mean rms differences at T31 resolution around each latitude circle. In order from top to bottom are NMC–ECMWF, twice versus four times daily, initialized versus uninitialized, 7 versus 14 levels, and 7 versus 20 levels, where the latter uses relative humidity instead of specific humidity for vertical interpolation.

Equation (4) may be vertically integrated to produce

$$\frac{\partial w}{\partial t} + \nabla \cdot \frac{1}{g} \int_0^{p_s} q\mathbf{v} dp = E - P, \qquad (6)$$

where E is the evaporation from the surface and P is the precipitation. In practice all the velocity fields are adjusted first so that the dry mass budget is satisfied (Trenberth 1991).

Over an annual cycle, the change in storage of moisture in the atmosphere is small. Over land, because there is a net runoff in streams, the precipitation must exceed the evaporation, so that $E - P$ should be negative on average. This constraint provides a weak check on any diagnostic results, although one which is typically not satisfied at all well, such as in the results of Peixoto and Oort (1983). More detailed constraints can be included where information exists on the actual runoff (e.g., Oki et al. 1993; Roads et al. 1994).

The first term in (6) is small for monthly or longer time averages so that it is the divergence of the vertically integrated atmospheric moisture flux that determines the net freshwater exchange with the surface. The moisture divergence can be written as

$$\nabla \cdot q\mathbf{v} = q\nabla \cdot \mathbf{v} + \mathbf{v}_\chi \cdot \nabla q, \qquad (7)$$

so that it can be broken up into contributions that depend mostly on the mass divergence in the lower atmosphere (where q is large) and horizontal advection by the divergent component of the wind ($\mathbf{v}_\chi$), which depends on gradients of q.

b. *Mean fields*

We define an overbar to be a finite time average and a prime to denote the departure from that mean, so that, for instance, $u = \bar{u} + u'$. Thus $\bar{u} = 1/N\sum_{i=1}^{N} u_i$, where there are N individual values u_i in the mean. Accordingly, covariances, such as between $\mathbf{v}$ and q, which give the moisture flux, can be expressed as $\overline{\mathbf{v}q} = \bar{\mathbf{v}}\bar{q} + \overline{\mathbf{v}'q'}$. Thus, when time averages are taken, the moisture flux can be divided into the mean and transient components.

All the mean and transient terms have been evaluated for use in both the time mean of (3) and (6) for individual months, and the results averaged to give the annual mean. Trenberth and Solomon (1994) present results for January, July, and the annual mean for 1988. The tendency term is small but has been included in each monthly mean calculation.

c. *Vertical integrals*

Although not required in (6), we have found by changing the number of p levels used that for any A, the $\partial A/\partial p$ terms are better evaluated in finite-difference form in $\ln p$ coordinates as $(1/p)(\partial A/\partial \ln p)$ using centered differences wherever possible. Then the vertical integral becomes $(1/g)\int_0^{p_s} A dp = (1/g)\int_0^{\ln p_s} pA d\ln p$.

In most cases the vertical integral is simply performed using values of q for the relevant pressure layer using a trapezoidal integration. In the global pressure analyses archive the vertical resolution in the boundary

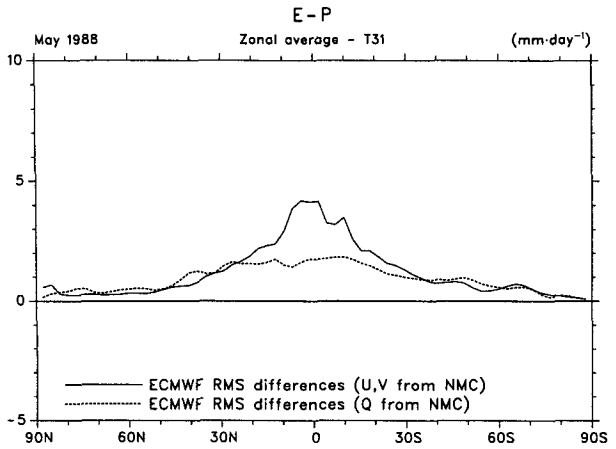

FIG. 4. Results of tests on $E - P$ for May 1988 in millimeters per day, where the q fields from ECMWF were combined with the velocity fields from NMC and vice versa compared with the ECMWF fields as rms differences at T31 resolution around each latitude circle.

layer, where most of the moisture is contained in the atmosphere, is poor. For q, this is especially critical as values fall off very rapidly and nonlinearly with height. On the other hand, the relative humidity RH is more uniform with height and is the preferred analysis quantity. Accordingly, in one case the working grid is changed from the coarse analysis levels 1000, 850, 700 mb . . . to a 50-mb layer thickness to which the RH, T, ω, and velocity fields are linearly interpolated in $\ln p$, and then q is calculated at these 20 levels at each time prior to computing monthly mean statistics. This is considered the most accurate calculation possible from the seven pressure levels of original information and is referred to as the "20 level" case.

4. Test computations

A number of tests have been made to determine the effects of different assumptions in the processing. Because the WMO archive from ECMWF consists of only seven levels and is initialized, while 14 or 15 levels of uninitialized analyses exist in the other archives either twice- or four-times daily, we assess the effects on precipitable water and the overall moisture budget as given by $E - P$ of

(i) 7-level versus 14-level data,
(ii) 7-level versus 20-level data,
(iii) initialized versus uninitialized data,
(iv) 2-times versus 4-times daily data,
(v) the source of the data, ECMWF versus NMC, using seven common levels.

All these tests were performed for May 1988. In addition we have assessed the impact of adding the 925-mb level to the dataset as a 15th level after January 1992.

The use of the full 19 model-level dataset at T106 resolution provides a check on the best calculations possible from ECMWF, and we compare with results achieved when the data are first truncated at T42 and with the results of the pressure-level calculations for July 1990 and January 1991. This also provides a check on the extent to which horizontal resolution may be an issue in these kinds of diagnostics.

Figure 2 presents the results of the tests for precipitable water for May 1988. At left is shown the bias in the zonal mean and at right is the root-mean-square difference around each latitude circle. The datasets were first truncated to T31 to ensure that the rms differences

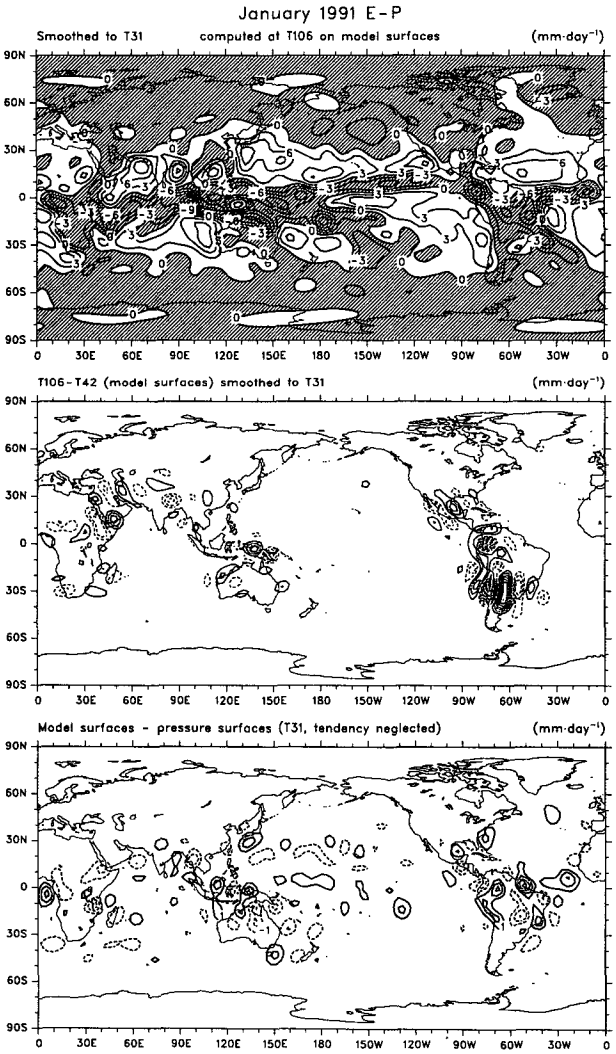

FIG. 5. For January 1991 $E - P$ from ECMWF computed at T106 resolution in model coordinates with final results truncated at T31, contour interval 3 mm day^{-1} (top); differences when all fields are first truncated at T42 (T106–T42) at T31 resolution, contour interval 0.25 mm day^{-1} (middle); and differences when the 14-level p archive is used, contour interval 1 mm day^{-1} (bottom). Negative values are shaded (top) or dashed, and the zero contour is omitted from the lower two panels.

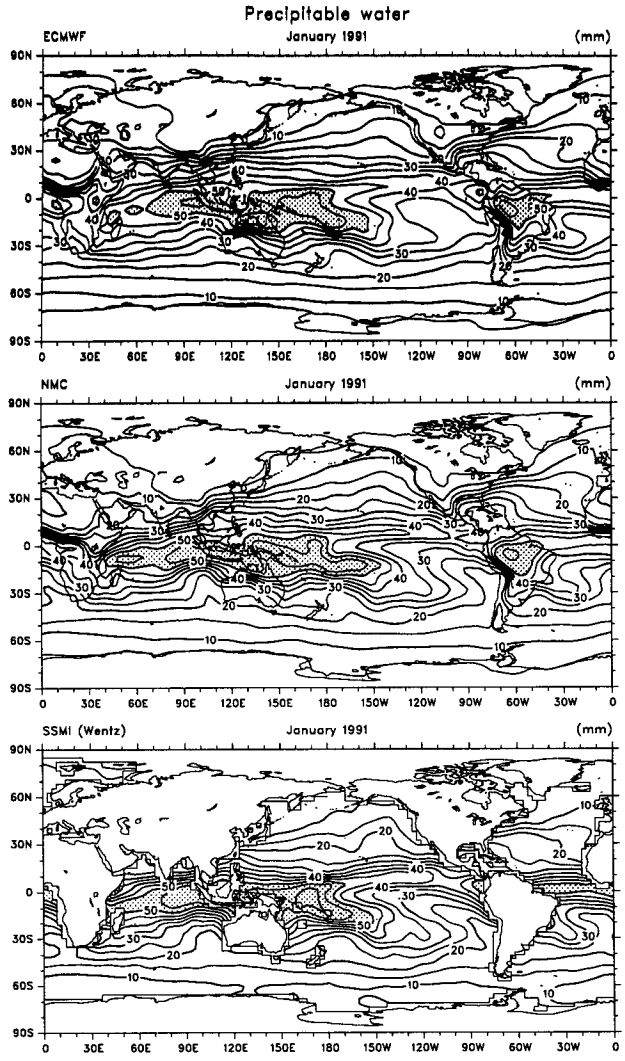

FIG. 6. The total precipitable water from ECMWF, NMC, and the Wentz SSM/I algorithm for January 1991. Values greater than 50 mm are stippled and the contour interval is 5 mm.

were not just on very small scales. For precipitable water initialization has no impact, not surprisingly. A small bias exists when 7 versus 14 levels are used in spite of the fact that the same levels are used in the lower half of the troposphere. When the 15th 925-mb level is added, a further small bias is revealed, and the global mean precipitable water is reduced by 0.15 mm. The bias is much larger in the 7- versus 20-level comparison showing that the use of specific humidity in place of relative humidity for vertical interpolation–integration leads to an overestimate of precipitable water. Not unexpectedly, differences from using 2-times versus 4-times daily data are more regional and the differences are ~0.5 mm throughout the Tropics. All these differences are small compared with the NMC–ECMWF bias and rms differences, which are typically 3 to 4 mm throughout the Tropics.

The results from the same tests for $E - P$ (Fig. 3) show that some of the systematic biases in total moisture have little impact, while other effects come into play, evidently because of the impact of the tests on the velocity field. In Fig. 3 the differences have been multiplied by L to give units of watts per squared meter, but these can be converted to millimeters per day by dividing by 29. Differences using 7 versus 14 or 20 levels are quite small. However, in contrast to Fig. 2, initialization has a noticeable effect because of the change in the divergence field, and the diurnal cycle emerges as very significant regionally, as seen by the 2- versus 4-times daily rms differences in $E - P$ of 1–2 mm day^{-1}. For May 1988 differences between NMC and ECMWF are typically 3 to 4 mm day^{-1} in the Tropics, which is almost as large as the quantity itself. This aspect is pursued further for all months below.

Tests were also run for May 1988 where the moisture fields from NMC and ECMWF were switched and merged with the velocity fields from the other center; $E - P$ was then computed to assess the extent to which the differences arose from q and w versus differences in moisture transport and divergence, as given in (7). The results are summarized in Fig. 4, and it is clear that it is the differences in $\mathbf{v}_\chi$, and especially $\nabla \cdot \mathbf{v}$, that is the primary source of the differences in $E - P$ in the Tropics. In the extratropics, the differences arise roughly equally from discrepancies in both winds and moisture.

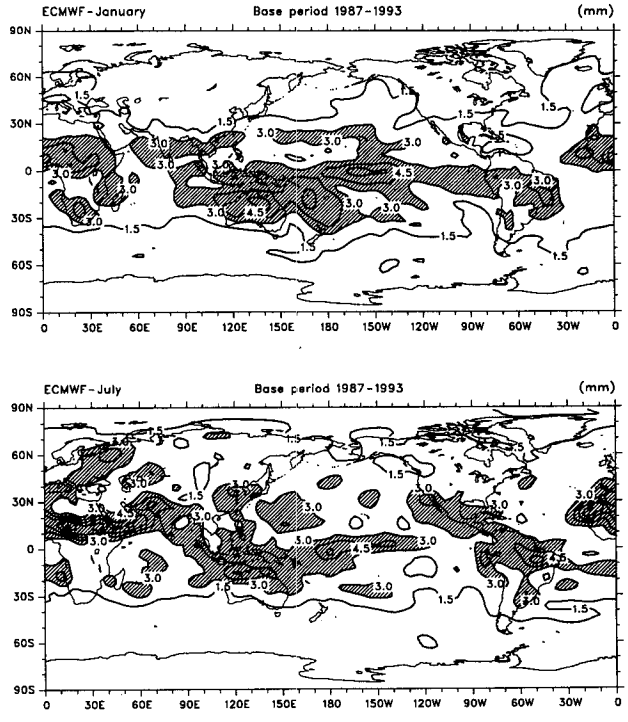

FIG. 7. The standard deviation of w from 1987 to 1993 (7 yr) from ECMWF for January and July. Values greater than 3 mm are hatched and the contour interval is 1.5 mm.

Calculations with the full 19 model levels at T106 resolution show that very little is lost in $E - P$ on the scales larger than T31 when the fields are first truncated at T42. Note that we have not included a comparison for precipitable water because of the disparity in the p_s fields. The $E - P$ results are illustrated for January 1991 in Fig. 5, which presents the results using the 19 level-model-coordinate data computation at T106 resolution with the final result truncated at T31. Also shown are the differences when all the fields, including the surface pressure, are first truncated at T42 and the differences when the computation is performed using the 14-level pressure archive. For convenience, none of these computations included the tendency term.

The result using T42 data differs by very small amounts from T106. Of course there are many very small-scale differences, but when truncated at T31, the differences range from 1.6 to -2.8 mm day^{-1} and with largest values in the immediate vicinity of the Andes and clearly associated with the topography. Evidently the change in p_s to lower resolution is a big factor in this area. Away from the Andes, largest differences are also found in association with steep topography in Central America, New Guinea, and the Ethiopian highlands, but all differences are small in scale, quite local, and less than 1 mm day^{-1} (rms differences around a latitude circle are ~0.2 mm day^{-1} from 40°N to 20°S). In July (not shown) differences are similar in magnitude, but in this season, as well as large differences in the proximity of the Andes, differences are also large in the Himalayan–Tibetan Plateau complex region. This result of relatively small and localized differences contrasts with the result of a similar comparison but for the heat budget (Trenberth et al. 1993; Trenberth 1995); however, the latter was evaluated locally in the vertical and it turns out that the greatest discrepancies arise from the vertical advection terms,

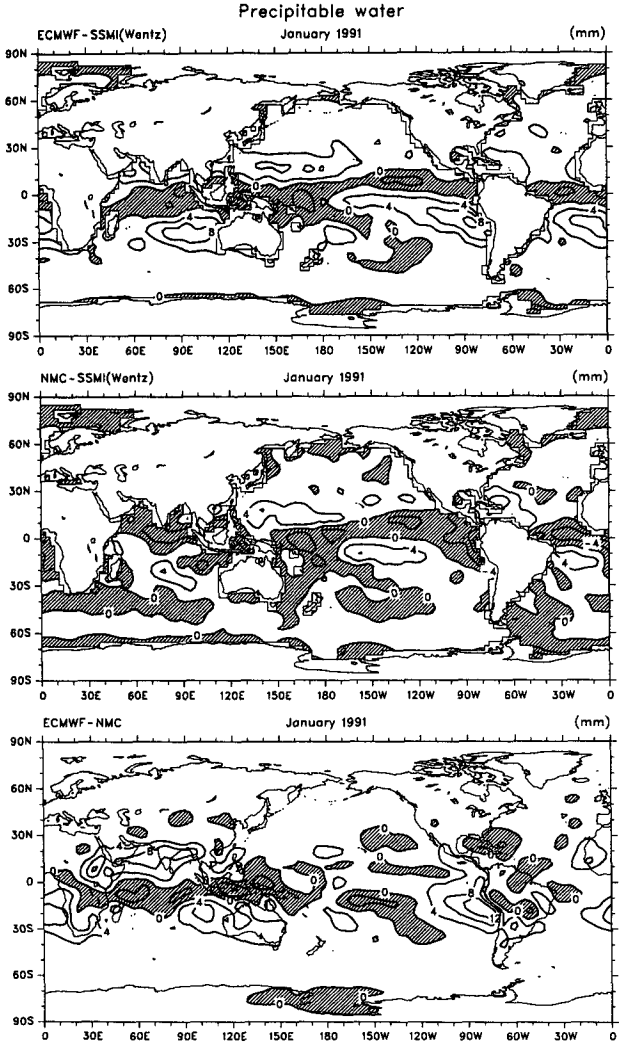

FIG. 8. For January 1991, the difference maps ECMWF-SSM/I (Wentz), NMC-SSM/I (Wentz), and ECMWF-NMC. Negative values are hatched and the contour interval is 4 mm.

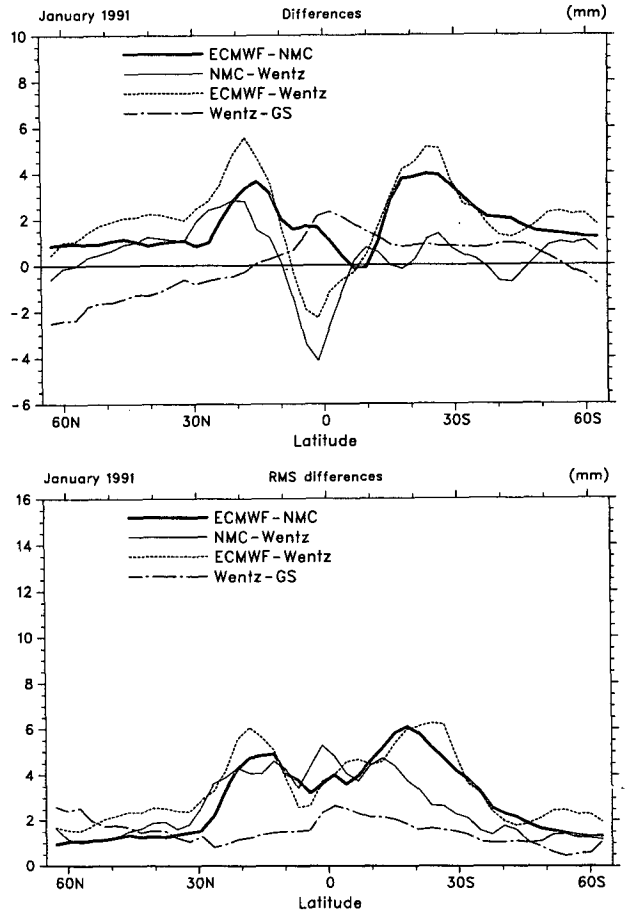

FIG. 9. For January 1991, the zonal mean and rms differences ECMWF-SSM/I (Wentz), NMC-SSM/I (Wentz), ECMWF-NMC, and Wentz-GS SSM/I as a function of latitude, where the differences are computed only over the common regions.

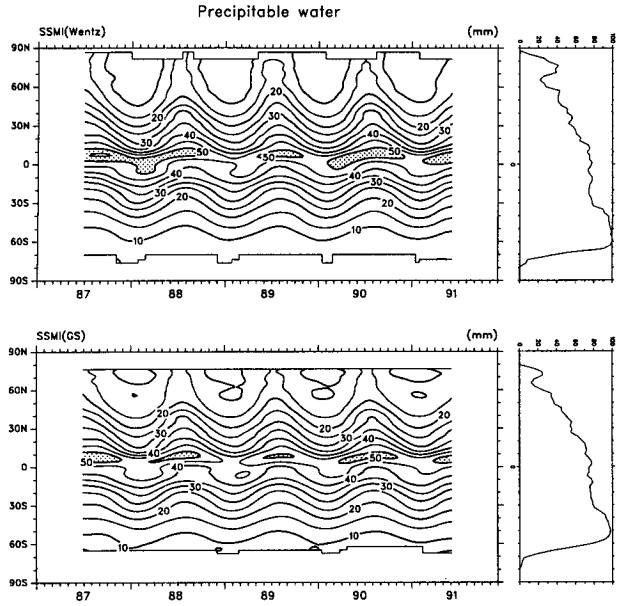

FIG. 10. The latitude–time sequence of the zonal ocean means of the Wentz and GS SSM/I w in mm, with the percentage of the latitude circle covered given at right.

which are avoided when the vertical integral is computed [see (4) to (6)].

Differences with the computations made in p coordinates (Fig. 5) for the same months reveal localized differences of up to 4 mm day^{-1}, although more typical differences are less than 1 mm day^{-1} (rms differences $\sim$0.9 mm day^{-1} in the Tropics). In this case, there is no obvious relation between the discrepancy and either steep topography or $E - P$ itself, although largest differences are over land. The same is true in July (not shown). Because of the vertical interpolation and limited number of levels, vertical resolution at low levels is the most likely source of these discrepancies.

An important conclusion from these experiments is that the horizontal resolution of the data is very important locally in the vicinity of steep orography, but it is *not* a big factor on large scales even where steep gradients exist in precipitation. Rather, the sources of any problems that exist (as shown further later) are in the large-scale analyzed fields of moisture and divergence themselves. Moreover, the general patterns can be captured quite well with analyses in p coordinates, although high resolution at low levels and proper treatment of p_s is vital for reliable results.

For the other months from 1987 to 1993, in view of the small impact of the method of vertical interpolation on the moisture budget, calculations were performed using q and all the available levels (14 or 15 from ECMWF, 12 from NMC) to make the best computation possible from each dataset.

5. Precipitable water comparisons

Precipitable water amounts from the Wentz algorithm have been extensively compared with radiosonde data and ECMWF analyses for July 1987 to July 1989 by Liu et al. (1992). That effort served to validate the SSM/I product while indicating areas of bias in the ECMWF analyses. Our results replicate those for the common period, but we update the comparison with more recent data and provide a longer-term perspective as a prelude to examining the moisture budget. In addition, we include the NMC and NASA/Goddard analyses in the comparison and the alternative GS SSM/I algorithm as a measure of uncertainty in the SSM/I product. The NASA/Goddard analyses are included in only limited ways and are not available for January 1991, featured below.

Figure 6 shows the total precipitable water from ECMWF, NMC, and the Wentz SSM/I algorithm for January 1991 (the most recent January available for SSM/I). The SSM/I data are available only over ocean regions. Qualitatively the fields are all quite similar, but there are quantitative differences. As a rough measure of the importance of real differences, the standard deviation of w from 1987 to 1993 (7 yr) from ECMWF for January and July is given in Fig. 7. Values exceed 3 mm throughout much of the Tropics. While part of the variability is spurious and arises from the analysis system changes, most of what is seen here is probably real and a substantial fraction is associated with changes in sea surface temperatures (SSTs), such as from ENSO

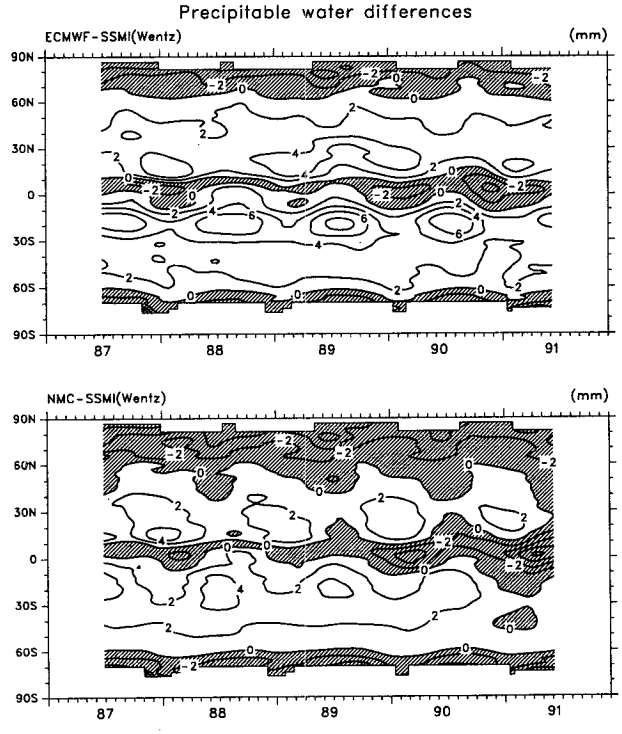

FIG. 11. The latitude–time sequence of the zonal ocean means of the differences between ECMWF and SSM/I (Wentz) (top) and NMC and NMC and SSM/I(Wentz) w in millimeters. Negative values are hatched and the contour interval is 2 mm.

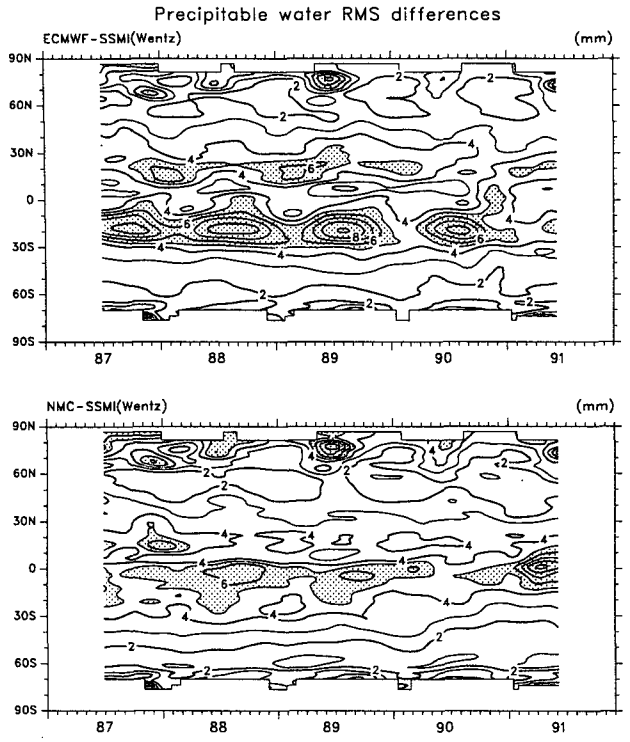

FIG. 12. The latitude–time sequence of the rms zonal ocean differences between ECMWF and SSM/I(Wentz) (top) and NMC and SSM/I(Wentz) w in millimeters. Values greater than 5 mm are stippled.

events. The standard deviation of w is similar in magnitude, although differing in spatial detail, for NMC.

Overall, the differences between w from the two SSM/I algorithms are relatively small, and so only the differences ECMWF − SSM/I(Wentz), NMC − SSM/I(Wentz), ECMWF − NMC, and Wentz − GS SSM/I are presented, although all results are summarized as zonal mean statistics later. For January 1991, the difference maps are given in Fig. 8, and Fig. 9 presents the zonal mean and rms differences as a function of latitude, where the differences are computed only over the common regions. The Wentz − GS SSM/I w zonal mean differences are 1–2 mm, with Wentz values higher from 10°N–50°S but lower north of 20°N. From 30°N–45°S all the other differences are typically much larger, 3 to 5 mm. Largest differences occur with the ECMWF analyses over the subtropical oceans, especially in the stratocumulus region off the west coast of South America.

Figure 10 presents the latitude–time sequence of the zonal ocean means of the Wentz and GS data, with the percentage of the latitude circle covered given at right. As was seen in Fig. 9, differences are most readily and consistently seen along the equator and at polar latitudes. Much larger differences, however, are generally found with ECMWF and NMC w (Fig. 11) and for the rms differences (Fig. 12). Changes with time in both differences are believed to result mainly from the multitude of changes in the ECMWF and NMC analysis systems. Because the SSM/I data were from a single satellite for the period of interest, changes from this source are believed to be small. These figures give a perspective on the January 1991 patterns presented earlier as being fairly typical. If anything, discrepancies with ECMWF were larger in the subtropics in earlier years. Note the positive biases in the subtropics and the negative biases in the intertropical convergence zone (ITCZ) regions in both analyses.

Correlations between ECMWF and Wentz values for all data, including the annual cycle, are shown in the top of Fig. 13. Aside from polar regions, the lowest correlation is at 15°S, 100°W and the time series for this point from ECMWF, GS, and Wentz are shown in the lower part of the figure. The mean ECMWF values in 1985 are much closer to the subsequent SSM/I values up until the time of the introduction of TOVS data into the analyses in early 1986. The bias of 10 mm or so was reduced by only a small amount in 1990, perhaps in association with changes in the 4DDA model evaporation at low wind speeds.

The large biases in the subtropics and especially in the region off South America were also found by Liu et al. (1992). These areas are essentially free from any

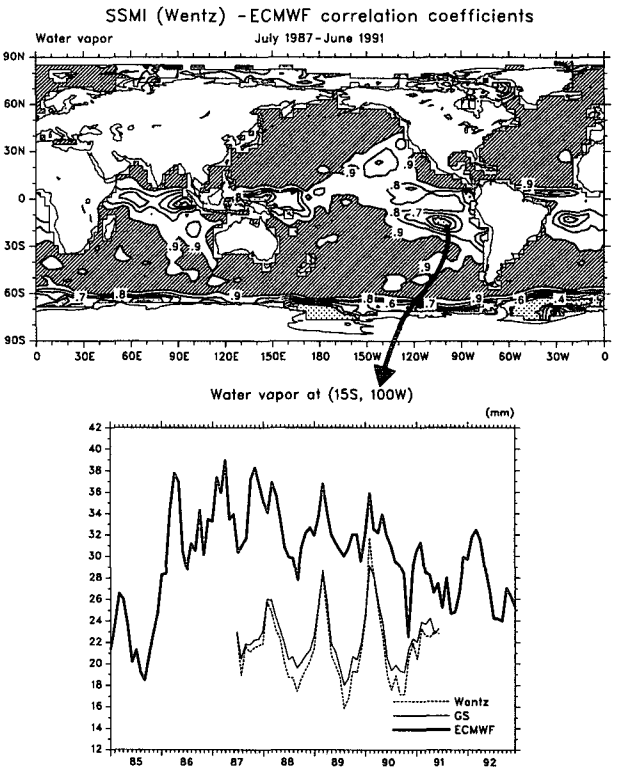

FIG. 13. Correlations between ECMWF and SSM/I(Wentz) w for all data including the annual cycle (top). Values greater than 0.9 are hatched. Time series at 15°S 100°W from ECMWF, SSM/I(GS), and SSM/I(Wentz) (bottom).

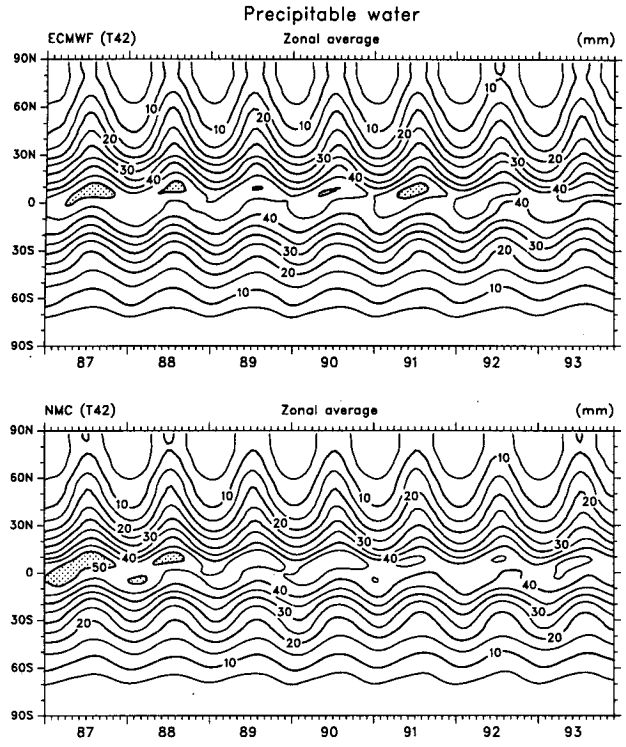

FIG. 14. NMC and ECMWF latitude–time series of zonal mean w for the whole globe. The contour interval is 5 mm.

conventional data, and the only source of information to the analyses is from the NWP model and TOVS satellite data. Wittemeyer and Vonder Haar (1994) evaluated the TOVS water vapor information and note the weaknesses of the TOVS w data in areas of cloud where data cannot be collected and that the "first guess" in the retrieval process is from land-based rawinsondes that are therefore biased over the oceans. They conclude that TOVS w are overestimated in dry subtropical high pressure cells by comparing with SSM/I data. Note that ECMWF has recently abandoned use of the TOVS retrievals and instead is using the radiance data, or strictly speaking TOVS brightness temperatures, directly in a variational analysis (Eyre et al. 1993).

We have also compared the Wentz SSM/I data for w with values from the NASA/Goddard reanalysis for July 1987 through 1989 (not shown). The NASA/Goddard analyses exhibit a distinctive dry bias, especially in the summer hemisphere. In July over the oceans the dry bias is about 2 to 6 mm over the Northern Hemisphere, and in January the dry bias exceeds 6 mm in the equatorial regions and is present from 10°N to 45°S. Values are especially low in the ITCZ in the NASA/Goddard analyses, and overall rms differences are larger than with NMC or ECMWF in the Tropics. The distinctive pattern of bias associated with the TOVS soundings is not present in the NASA/Goddard analyses.

The full NMC and ECMWF latitude–time series for the whole globe (not just oceans) is given in Fig. 14, and the differences (zonal mean and rms) are given in Fig: 15. In the Tropics both analyses have become drier with time, and the NMC analysis became much drier in early 1991 in association with the introduction of the T126 model in the 4DDA system (6 March 1991) and the Spectral Statistical Interpolation (SSI) analysis system (25 June 1991). As indicated in Fig. 11, relative to the SSM/I, these changes made the analyses much worse. However, the NMC and ECMWF zonal mean analyses became more similar again in 1992 as the ECMWF analyses underwent a drying in June 1992 when the SYNOP humidity data were rejected specifically "to reduce excessive convective precipitation in short and early medium-range forecasts," to quote the September 1992 *ECMWF Newsletter*. The biggest effects of this change were found over the tropical continents of South America and Africa in the very low troposphere. There is no reason to believe that this change was an improvement in the analyses, although it alleviated some problems in generating the forecast.

Relative to the short climatology for 1987 to 1991 from SSM/I(Wentz), the January 1993 ECMWF analysis (not shown) contains negative biases throughout the tropical convergence zones of 4 to 16 mm, while the positive bias remains off South America and in the subtropical highs. In fact the ECMWF analyses

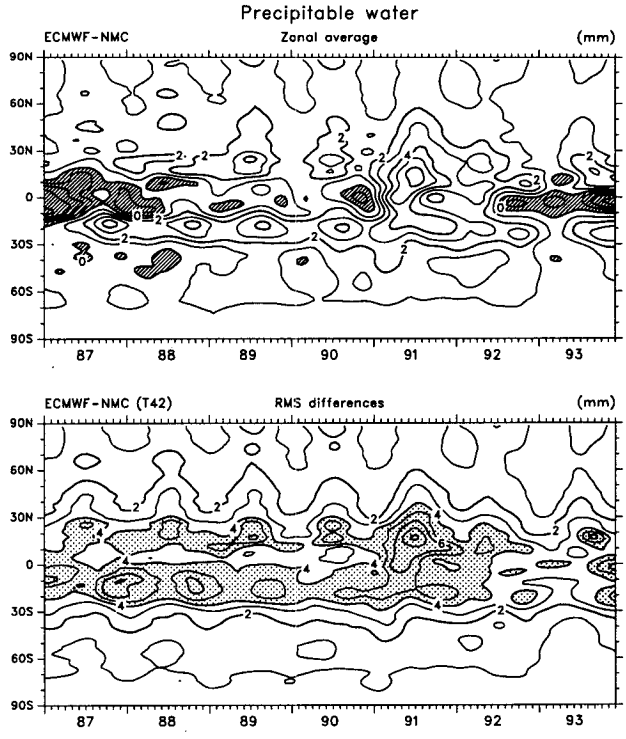

FIG. 15. NMC and ECMWF latitude–time series of zonal mean and rms w differences (mm). Negative values are hatched (top) and values greater than 4 mm are stippled in the lower panel.

are drier than NMC in the deep Tropics. In July 1993, the negative tropical bias (not shown) is not so large (1 to 8 mm), but the positive subtropical bias is somewhat larger (typically 4 to 8 mm). There is no indication in the period we have examined that the analyses from either center are becoming closer to the "truth" as given by the SSM/I fields.

6. Evaporation–precipitation budget comparisons

The moisture budget comparison is restricted to the residual $E - P$ estimates. An examination of the monthly mean E and P fields for 1987 to 1989 from the NASA/Goddard reanalysis reveals that standard deviations of the monthly means for the Tropics and subtropics are typically 0.5 mm day^{-1} for E over extensive areas, but several millimeters per day for P over only those areas where the tropical convergence zones and monsoon rains are active. Mean values of E exhibit much less spatial structure than P and average about 3 to 5 mm day^{-1} over most of the Tropics and subtropics (Fig. 16). It is clear that $E - P$ temporal monthly variability is dominated by variations in location and intensity of rainfall and that the spatial structure in $E - P$ is also dominated by the P field.

As well as showing the E and P fields from NASA/Goddard for July 1988, Fig. 16 presents $E - P$ from the residual calculation using ECMWF analyses and the P field from the GPCP data. These will be discussed further below as the characteristics of the $E - P$ fields are identified from NMC and ECMWF.

Figure 17 presents the zonal mean $E - P$ from both ECMWF and NMC as a function of latitude and time from 1987 to 1993. Note the strengthening in the excess of P in the deep Tropics after May 1989 for ECMWF, corresponding to the model change at that time (cf. Fig. 1) to peak values in excess of 6 mm day^{-1} for $P - E$, values larger than indicated for NMC. The differences (Fig. 18) are seen to be up to 3 mm day^{-1} for the zonal means in the tropical convergence zone and typically 3 to 5 mm day^{-1} in an rms sense.

To see where these differences are coming from, the total fields are presented for January and July 1993 along with differences in Figs. 19 and 20 at T31 resolution. This reveals the tendency for somewhat stronger and more localized values in the ECMWF results, so that the differences tend to be quite spotty. Thus, although the very broad-scale patterns of the fields are quite similar, the localized differences can be very large in places where heavy rain is indicated in one but not the other analysis. The summary for these months is shown in Fig. 21 with both the mean and rms differences compared with the rms values of the field itself

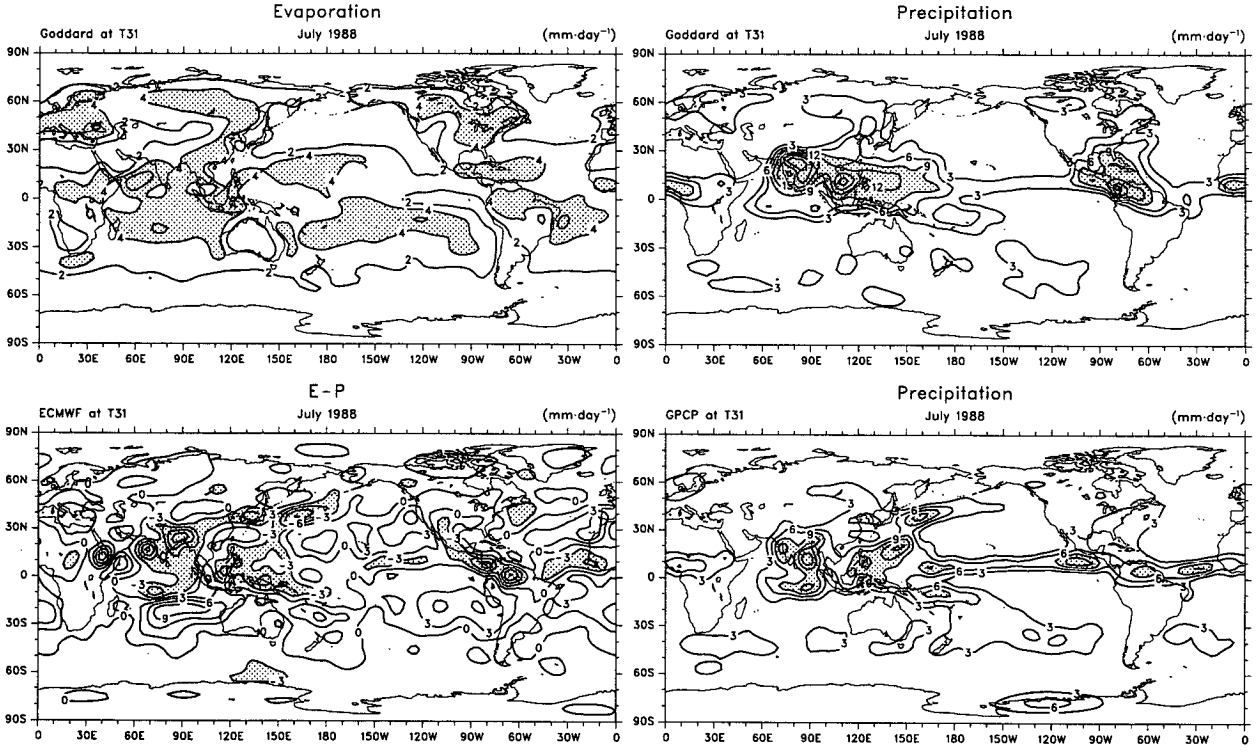

FIG. 16. For July 1988 presented are E (top left) and P (top right) from the NASA/Goddard reanalysis, $E - P$ from ECMWF (lower left), and P from the GPCP project (lower right). All values are in millimeters per day. For E the contour interval is 2 mm day^{-1}, and values exceeding 4 mm day^{-1} are stippled. For P the contour interval is 3 mm day^{-1} and values exceeding 9 mm day^{-1} are stippled. For the $E - P$ differences the contour interval is 3 mm day^{-1} and values less than -3 mm day^{-1} are stippled.

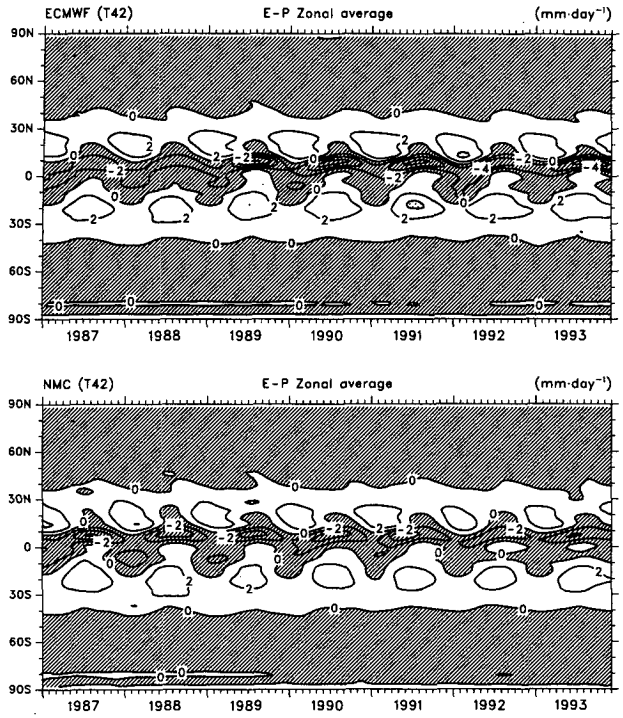

FIG. 17. The latitude–time sequence of the zonal mean $E - P$ from ECMWF (top) and NMC (bottom). Negative values are hatched and the contour interval is 2 mm day^{-1}.

from ECMWF. The latter may be taken as a measure of the signal of interest and is typically 4–5 mm day^{-1} in the Tropics, while the rms difference can be considered as the noise of typically 3 mm day^{-1}. Thus, the level of noise is about 60%–75% of the signal in this field at T31 resolution and has not changed much with time. In spite of this noise, the fields do have a strong large-scale resemblance, and we have explored this by also calculating the rms differences at other resolutions. For example at T15 truncation, the rms differences (not shown) are remarkably close to being one-half of the rms differences at T31 resolution, that is, ~1.5 mm day^{-1} in the Tropics and about 30% of the signal.

The annual mean for 1993 for each analysis is presented in Fig. 22. This year is chosen solely because it is the most recent available, and the annual mean is of interest because by neglecting changes in atmospheric storage (which can be considered small), an assessment can be made over land as to whether the constraint that $P > E$ is satisfied in most places (the possible exceptions being places with sources of ground moisture such as lakes or rivers). Clearly there are large areas over Africa and southern Asia and parts of Australia and South America where even this modest constraint is violated by both analyses. The stronger precipitation in the tropical convergence zones is seen in the ECMWF analyses and is associated with the stronger low-level convergence and divergent circulation that occurred after the May 1989 changes (Fig. 1).

Overall correlation coefficients between the monthly mean NMC and ECMWF time series from January 1987 to December 1993 with the annual cycle included (not shown) exceed 0.8 mostly from 30° to 80°N and over the subtropical oceans of the Southern Hemisphere, but they are often less than 0.3 in the Tropics, throughout Africa and South America, and over Antarctica. Correlations are also low over the Rocky Mountain and Himalayan regions. Thus, the areas of largest discrepancies can be identified as areas of significant topography and regions of poor data coverage.

We now return to an overall evaluation of the $E - P$ fields by making use of the E and P fields, such as shown in Fig. 16, and for the other months in 1987 and 1988 for which we have P fields from the GPCP and NASA/Goddard analyses. We first made a direct qualitative comparison between the GPCP and NASA/Goddard P fields and then compared $E - P$ from NASA/Goddard, NMC, and ECMWF. All fields were first truncated at T31. While we treat the GPCP as a form of "truth," we note a problem feature over Antarctica where p exceeds 6 mm day^{-1}! We do not present the NMC results, and it is important to note that the characteristics of both ECMWF and NMC analyses are quite different in 1987–1988 than shown in Figs. 19, 20, and 22 for recent years. Prior to 1989 the ECMWF rainfall was not so intense, while the NMC fields were considerably more intense and featured

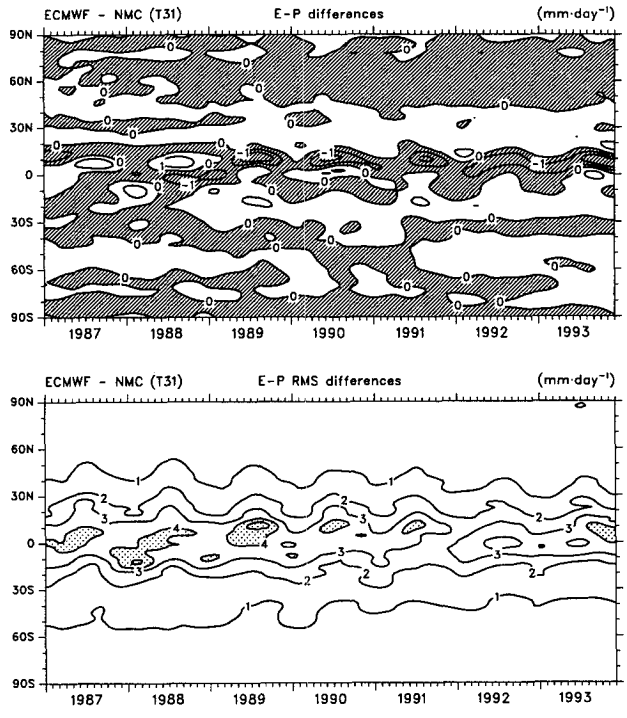

FIG. 18. The latitude-time sequence of the monthly mean $E - P$ zonal mean (top) and rms differences (bottom) between ECMWF-NMC. Negative values are hatched, the contour interval is 1 mm day^{-1}, and values exceeding 4 mm day^{-1} are stippled.

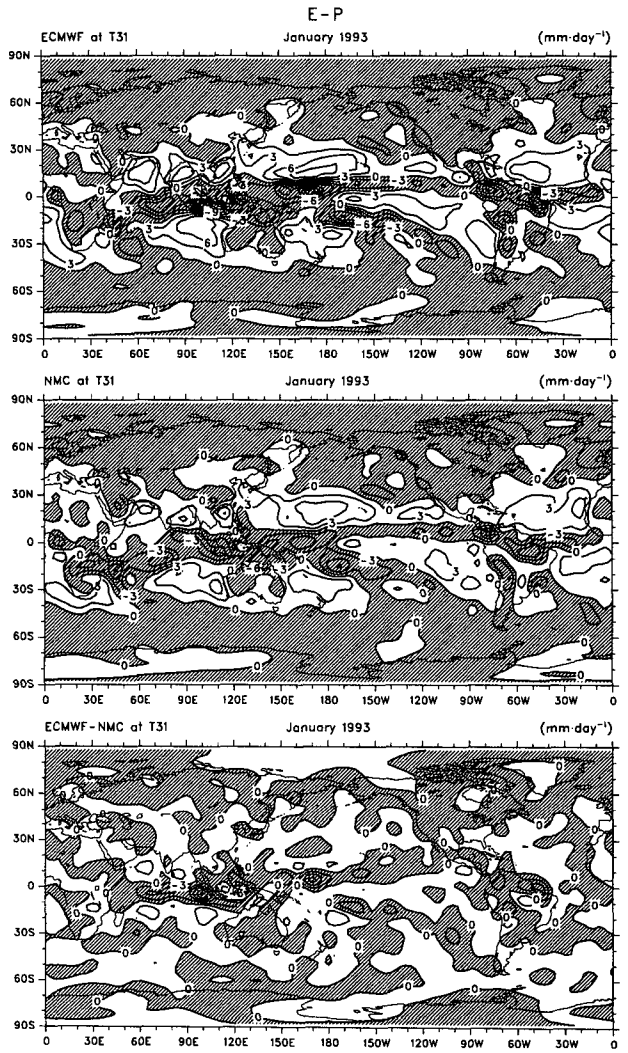

FIG. 19. $E - P$ for January 1993 at T31 resolution from ECMWF (top), NMC (middle), and their difference ECMWF-NMC (bottom). Negative values are hatched and the contour interval is 3 mm day^{-1}.

stronger bullseye features. For the ECMWF $E - P$ field in Fig. 16, the stippled region is selected to correspond very roughly with the stippled regions in the panels for P alone.

The wintertime Northern Hemisphere storm track is very well depicted in the NASA/Goddard analyses (not shown), although the storm track is a bit weak in the Southern Hemisphere. However, in the northern summer, the rainfall maximum off of Japan is largely absent in the NASA/Goddard analyses (Fig. 16), although very well represented in the NMC and ECMWF analyses. In the Tropics there is far too much precipitation implied in all three analyses over land in Central America, and this tends to be the case also over southern Asia and over the Ethiopian highlands for NMC and ECMWF. The NASA/Goddard ITCZ is much too weak in both the Atlantic and the Pacific, and the implied P values in the NMC and ECMWF analyses are closer to those from GPCP. In general, the NMC fields in 1987 and 1988 exhibited the strongest features, but with maxima often in the wrong place and too strong compared with the GPCP. The NMC fields became quite a bit weaker, closer in magnitude, and with a reduced problem in the landlocking of precipitation after the introduction of the T126 model and SSI system in 1991. Subjectively for 1987 and 1988, the ECMWF fields look to be closest to the GPCP, especially in the northern winter. However, the ECMWF fields have become much more intense with time (cf. Fig. 22), and the implication is there would be less agreement with the GPCP after May 1989. In Fig. 22 it is apparent that the erroneous tendency for too much landlocked precipitation over Central America is still present in the most recent analyses at both centers.

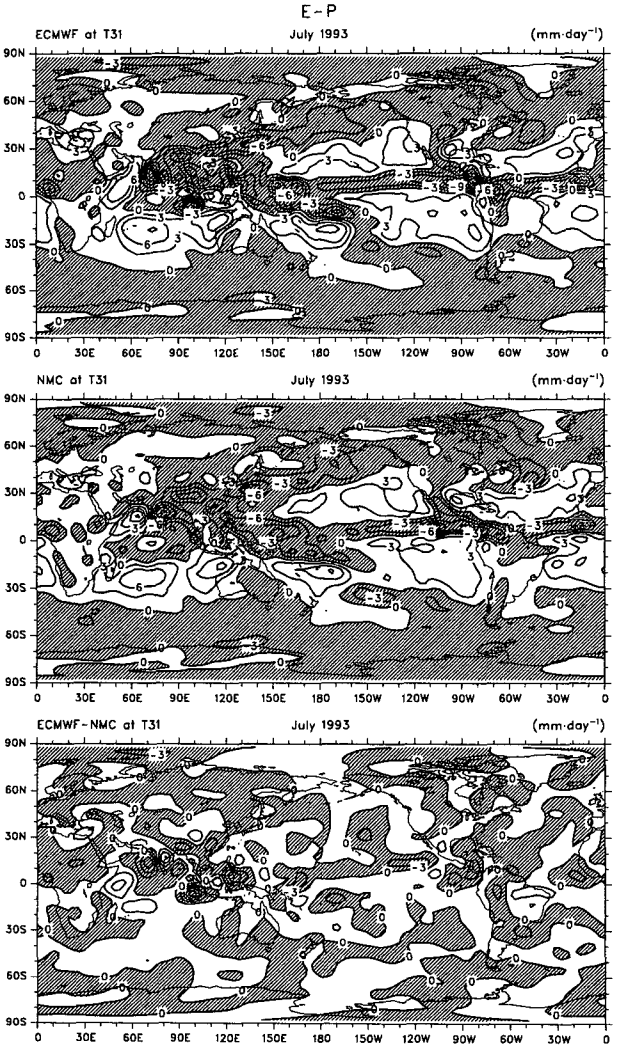

FIG. 20. $E - P$ for July 1993 at T31 resolution from ECMWF (top), NMC (middle), and their difference ECMWF-NMC (bottom). Negative values are hatched and the contour interval is 3 mm day^{-1}.

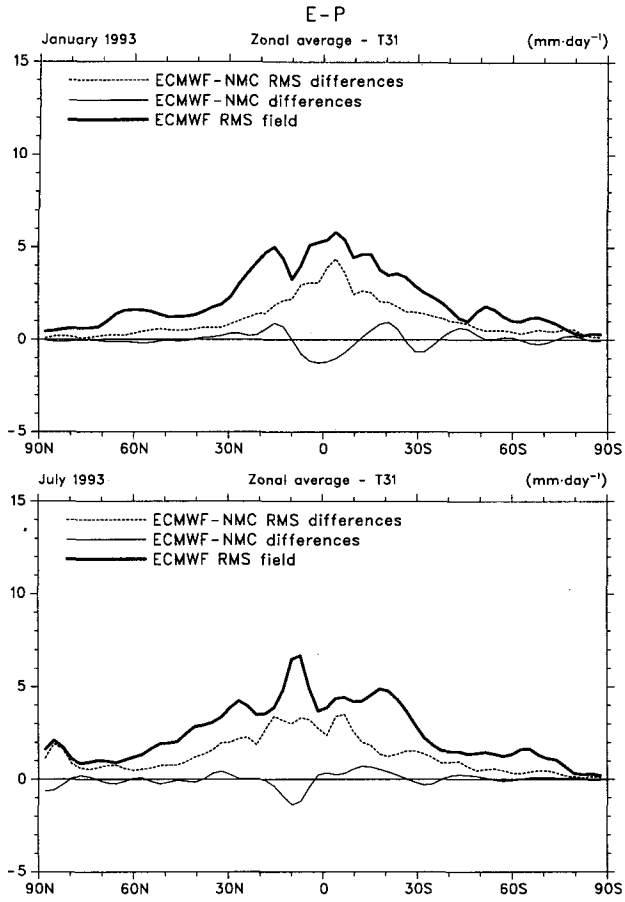

FIG. 21. $E - P$ meridional profiles of ECMWF rms values (thick line), ECMWF-NMC zonal means (thin line), and ECMWF-NMC rms differences (dashed) in mm day^{-1} for January (top) and July (bottom) 1993.

7. Discussion and conclusions

We have documented results of tests performed on the sensitivity of w and $E - P$ to vertical resolution, diurnal sampling, and several other things. In the Tropics, the tests have highlighted the dependence of the moisture budget on the veracity of the velocity field and specifically on the horizontal divergence. In the midlatitudes, quasigeostrophic dynamics ensure that the divergence field is better known, and uncertainties in the moisture budget stem roughly equally from discrepancies in moisture analyses and the velocity field. Biases exist in w with vertical resolution, and vertical interpolation of q rather than RH tends to overestimate the moisture content of layers. However, the errors are systematic and do not have much effect on the moisture budget. Initialization has a substantial effect on the divergence field, as has been well known. It cuts down on noise but probably also cuts down the magnitude of the signal, so that it impacts the moisture budget significantly. The diurnal cycle is not well captured by twice-daily data, and, while not so important in w, it does make significant differences in $E - P$. Regionally, such as over the United States in summer, the diurnal cycle is known to be very important (e.g., Helfand and Schubert 1995).

With the advent of SSM/I fields that have been validated with radiosonde data (e.g., Liu et al. 1992), an accepted truth exists for precipitable water over the oceans that can be used to validate the global analyses from NMC and ECMWF. These data are not available in real time and so are not incorporated into the analyses. Instead TOVS retrievals have been extensively used, but several evaluations have shown them to be of limited or even negative value to the analyses (see Liu et al. 1992; Eyre et al. 1993; Wittmeyer and Vonder Haar 1994). Large positive biases are evident in the subtropics and especially in the region off South America in the ECMWF analyses. In several respects the NMC and ECMWF analyses are more like each other than either are like the SSM/I. This may be related to the 4DDA methods and the underlying models used. Schmetz and van de Berg (1994) have shown using the Meteosat water vapor channel that depicts water vapor in the mid- to upper troposphere that the ECMWF model 12–24-h forecast fields for July 1992 are slightly too dry in the tropical convergence zone and significantly too moist in the subtropical regions over the South Atlantic and northern Africa—conclu-

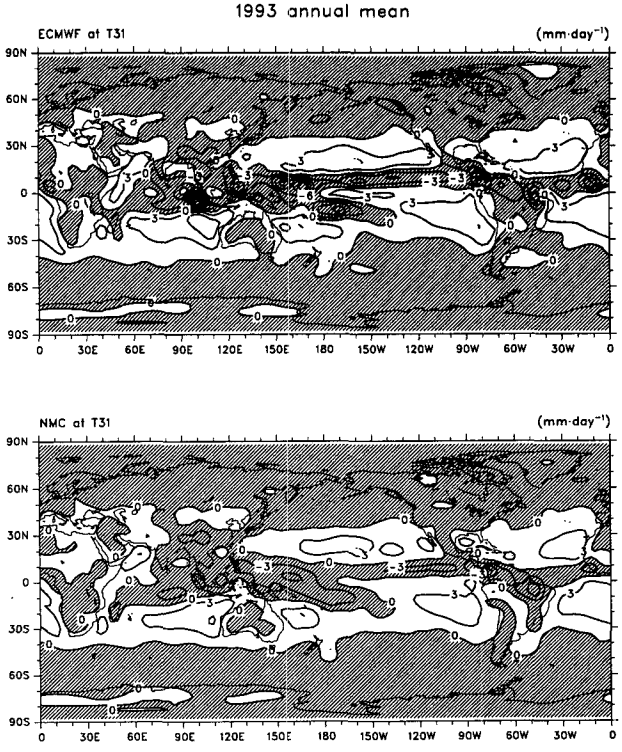

FIG. 22. Annual mean $E - P$ for 1993 at T31 resolution from ECMWF (top) and NMC (bottom). Negative values are hatched and the contour interval is 3 mm day^{-1}.

sions compatible with the results of Soden and Bretherton (1994). In these regions the precipitable water above 500 mb in the model is as much as twice that inferred from satellite. Schmetz and van de Berg (1994) also note that these biases are not associated with model spinup as the same biases are evident for 36-h as with 12-h forecasts. The conclusion is that the analyses tend to be dominated by the characteristics of the NWP model climate in the 4DDA and that biases are present (see also Norquist and Chang 1994). It appears that insufficient account is taken of the data that are available and that the 4DDA system is not capable of exploiting the data because of the inherent incompatibility with the NWP-assimilating model.

Calculations with the full 19 model levels at T106 resolution show that very little is lost in $E - P$ on the scales larger than T31 when the fields are first truncated at T42. The horizontal resolution of the data is very important locally in the vicinity of steep orography but not on large scales. As shown here, the sources of the problems that exist are in the large-scale analyzed fields of moisture and divergence themselves, which are in turn related to the parameterization of moist processes in the NWP model. We also showed that the general patterns can be captured quite well with analyses in p coordinates, although high resolution at low levels and proper treatment of p_s is vital for reliable results.

There is no acknowledged source of "truth" for $E - P$. We used the NASA/Goddard reanalyses to show that variability of E is much less than that of P, so that the main variations in $E - P$ in both space and time arise from the P variations. Under the GPCP project, global fields of precipitation are being assembled, but their availability is limited to a few months at present. Nevertheless, indications are that none of the global analyses produce very reliable results for the moisture budget at present. The differences between NMC and ECMWF are substantial and are traceable mostly to the continuing differences in the divergent circulation in the global analyses. Several methods exist for estimating evaporation using spaceborne sensors (e.g., Liu 1988), and it may eventually be worthwhile combining all the estimates of E, P, and $E - P$ to obtain the best estimates of these components of the hydrological cycle, but such an exercise seems premature at this point given that there are rms discrepancies of 60% to 75% in the current estimates of $E - P$ at T31 resolution.

The technique of using annual mean $E - P$ from atmospheric residual calculations and comparing to runoff has been carried out by Oki et al. (1993) for each of 35 major river basins for 1985 to 1988 ECMWF data. They found atmospheric moisture divergence (i.e., the wrong sign) in seven cases and discrepancies of up to 5656. For only 23 river basins was the error within 100%, and the agreement cannot be said to be good. In fact, our analysis suggests that the agreement between differing estimates of the atmospheric moisture convergence over complex terrain is poor. In part, this may be because of the treatment of the lower boundary in the NWP models and the use of envelope orography. Somewhat better results are achieved over the United States (Roads et al. 1994), where a very good rawinsonde network helps define the moisture transports, although still not without substantial corrections to the atmospheric moisture divergence. Over the oceans, Chen et al. (1994) have used the atmospheric moisture divergence to estimate the freshwater budget for the oceans using NMC data for 1979–1992, and they have found some agreement with oceanic estimates of Wijffels et al. (1992) but with considerably different magnitudes.

Activities are underway at NMC and ECMWF to reanalyze retrospectively the observations based upon state of the art 4DDA systems at each center. ECMWF will no longer use envelope orography during that exercise; however, it is apparent that the recent analysis systems continue to produce quite different products for moisture and large-scale atmospheric divergent circulation. Although the prospect may exist for using SSM/I data in the future and ECMWF does plan to use a new variational scheme for the 4DDA, it seems likely that the differences seen above for 1993 may also be present in the reanalysis products.

We conclude that there is enormous scope for improving our knowledge of and modeling ability for the global atmospheric hydrological cycle.

Acknowledgments. The ECMWF data used were provided by ECMWF. We thank Tim Liu for supplying the Wentz SSM/I data, Tom Greenwald for the GS SSM/I data, and Phil Arkin and Pingping Xie for the GPCP data. Dennis Shea and Jeff Berry provided help with the datasets. We also thank Rick Rosen for comments. This research is partly sponsored by the Tropical Oceans Global Atmosphere Project Office under Grant NA87AANRG0208 and NASA under NASA Order No. W-18,077.

REFERENCES

Arkin, P. A., and P. Xie, 1994: The Global Precipitation Climatology Project: First algorithm intercomparison project. *Bull. Amer. Meteor. Soc.*, **75**, 401–419.

Chen, T.-C., J. Pfaendtner, and S.-P. Weng, 1994: Aspects of the hydrological cycle of the ocean–atmosphere system. *J. Phys. Oceanogr.*, **24**, 1827–1833.

Eyre, J. R., G. A. Kelly, A. P. McNally, E. Andersson, and A. Persson, 1993: Assimilation of TOVS radiance information through one-dimensional variational analysis. *Quart. J. Roy. Meteor. Soc.*, **119**, 1427–1464.

Glantz, M. H., R. W. Katz, and N. Nicholls, Eds., 1991: *ENSO Teleconnections Linking Worldwide Climate Anomalies: Scientific Basis and Societal Impact.* Cambridge University Press, 535 pp.

Greenwald, T. J., G. L. Stephens, T. H. Vonder Haar, and D. L. Jackson, 1993: A physical retrieval of cloud liquid water over the global oceans using SSM/I measurements. *J. Geophys. Res.*, **98**, 18 471–18 488.

Helfand, H. M., and S. D. Schubert, 1995: Climatology of the simulated Great Plains low-level jet and its contribution to the con-

tinental moisture budget of the United States. *J. Climate,* **8,** 784–806.

Liu, W. T., 1988: Moisture and latent heat flux variabilities in the tropical Pacific derived from satellite data. *J. Geophys. Res.,* **93,** 6749–6760.

——, W. Tang, and F. Wentz, 1992: Precipitable water and surface humidity over global oceans from Special Sensor Microwave Imager and European Centre for Medium-Range Weather Forecasts. *J. Geophys. Res.,* **97,** 2251–2264.

Mo, K.-C., and E. M. Rasmusson, 1990: Atmospheric water vapor transport as evaluated from NMC analyses. *Proc. 15th Climate Diag. Workshop,* Asheville, NC, NOAA, 308–313.

Norquist, D. C., and S. S. Chang, 1994: Diagnosis and correction of systematic humidity error in a global numerical weather prediction model. *Mon. Wea. Rev.,* **122,** 2442–2460.

Oki, T., K. Musiake, K. Masuda, and H. Matsuyama, 1993: Global runoff estimation by atmospheric water balance using ECMWF data set. *Macroscale Modelling of the Hydrosphere, Proc. of the Yokohama Symp.,* Int. Assoc. Hydrol. Sci., 163–171.

Peixoto, J. P., and A. H. Oort, 1983: The atmospheric branch of the hydrological cycle and climate. *Variations in the Global Water Budget,* A. S. Perrott et al., Eds., D. Reidel, 5–65.

Roads, J. O., S.-C. Chen, A. K. Guetter, and K. P. Georgakakos, 1994: Large-scale aspects of the United States hydrological cycle. *Bull. Amer. Meteor. Soc.,* **75,** 1589–1610.

——, ——, J. Kao, D. Langley, and G. Glatzmaier, 1992: Global aspects of the Los Alamos General Circulation Model hydrologic cycle. *J. Geophys. Res.,* **97,** 10 051–10 068.

Rosen, R. D., and D. A. Salstein, 1980: A comparison between circulation statistics computed from conventional data and NMC Hough analyses. *Mon. Wea. Rev.,* **108,** 1226–1247.

——, and ——, 1985: Effect of initialization on diagnoses of NMC large-scale circulation statistics. *Mon. Wea. Rev.,* **113,** 1321–1337.

Savijärvi, H. I., 1988: Global energy and moisture budgets from rawinsonde data. *Mon. Wea. Rev.,* **116,** 417–430.

Schmetz, J., and L. van de Berg, 1994: Upper tropospheric humidity observations from Meteosat compared with short-term forecast fields. *Geophys. Res. Lett.,* **21,** 573–576.

Schubert, S. D., R. B. Rood, and J. Pfaendtner, 1993: An assimilated dataset for earth science applications. *Bull. Amer. Meteor. Soc.,* **74,** 2331–2342.

Simmons, A. J., and D. M. Burridge, 1981: An energy and angular-momentum conserving vertical finite-difference scheme and hybrid vertical coordinates. *Mon. Wea. Rev.,* **109,** 758–766.

——, and R. Strüfing, 1983: Numerical forecasts of stratospheric warming events using a model with a hybrid vertical coordinate. *Quart. J. Roy. Meteor. Soc.,* **109,** 81–111.

Soden, B. J., and F. P. Bretherton, 1994: Evaluation of water vapor distribution in general circulation models using satellite observations. *J. Geophys. Res.,* **99,** 1187–1210.

Trenberth, K. E., 1991: Climate diagnostics from global analyses: Conservation of mass in ECMWF analyses. *J. Climate,* **4,** 707–722.

——, 1992: Global analyses from ECMWF and atlas of 1000 to 10 mb circulation statistics. NCAR Tech. Note NCAR/TN-373+STR, 191 pp., 24 fiche.

——, 1995: Truncation and use of model-coordinate data. *Tellus,* **47A,** 287–303.

——, and J. G. Olson, 1988a: Intercomparison of NMC and ECMWF global analyses: 1980–1986. NCAR Tech. Note. NCAR/TN-301+STR, 81 pp.

——, and ——, 1988b: An evaluation and intercomparison of global analyses from NMC and ECMWF. *Bull. Amer. Meteor. Soc.,* **69,** 1047–1057.

——, and A. Solomon, 1993: Implications of global atmospheric spatial spectra for processing and displaying data. *J. Climate,* **6,** 531–545.

——, and ——, 1994: The global heat balance: Heat transports in the atmosphere and ocean. *Climate Dyn.,* **10,** 107–134.

——, J. C. Berry, and L. E. Buja, 1993: Vertical interpolation and truncation of model-coordinate data. NCAR Tech. Note NCAR/TN-396+STR, 54 pp.

Wijffels, S. E., R. W. Schmitt, H. L. Bryden, and A. Stigebrandt, 1992: Transport of freshwater by the oceans. *J. Phys. Oceanogr.,* **22,** 155–162.

Wittmeyer, I. L., and T. H. Vonder Haar, 1994: Analysis of the global ISCCP TOVS water vapor climatology. *J. Climate,* **7,** 325–333.

Yanai, M., S. Esbensen, and J.-H. Chu, 1973: Determination of bulk properties of tropical cloud clusters from large-scale heat and moisture budgets. *J. Atmos. Sci.,* **30,** 611–627.